JOURNAL OF MATERIALS SCIENCE 24 (1989) 2358–2368

Mechanisms of stable crack growth in ductile polycarbonate

P. S. THEOCARIS, V. KYTOPOULOS
Department of Engineering Sciences, Athens National Technical University, P.O. Box 77230 Athens, (175-10) Greece

An extensive study of the phenomena appearing during crack propagation in ductile polycarbonate during the phase of stable crack growth (SCG) was undertaken. It has been shown that this phase starts at a critical loading step where a blunted crack was established and a damaged ligament in front of the crack tip developed and stabilized. This phase may be divided into two successive steps. The first is characterized by the step by step advancement of the blunted crack by exhausting respective parts of the damaged ligament so that the overall length of crack and ligament remains stationary. In this step the crack tip opening angle is increasing and attains its final value of the order of 55 degrees.

This progressive crack growth, at the expense of the damaged ligament, is replaced by the proper steady crack growth where the crack advances steadily under almost constant external load and under constant CTOA up to a limit where catastrophic fracture occurs. The influence of the in-plane and transverse constraint factors was studied and important results concerning the mechanisms of fracture under predominating plane-stress or plane-strain conditions were established.

1. Introduction

A distinct phase of stable crack growth (SCG) lying between the onset of crack propagation and unstable crack growth is often observed during fracture of materials of various geometries [1–3]. Since stable crack growth occurs frequently and is often extensive, it is important to study the influence of this intermediate phase on the entire crack growth process.

Stable crack growth is usually accompanied by a steadily increasing crack driving force often represented either by the value of the stress intensity factor, K, or the value of the J integral, or the value of the crack-tip opening displacement (COD). This study gives rise to the resistance curve, or R curve, which is a plot of the driving force against the amount of stable crack growth (SCG). It is indicated that SCG is a feature inherent to elastic-plastic materials [4, 5].

To study the phenomenon a large number of theoretical and experimental investigations were undertaken. Older and more recent theoretical studies of SCG were concerned with the two extreme states of loading of cracked plates under conditions of small scale yielding, that is plane-strain and plane-stress conditions. Cherepanov [6] and Drucker and Rice [7] were among the list to study the SCG-phenomenon under conditions of plane stress by also considering the formation of a plastic Dugdale type zone in front of the crack tip. Later Rice and Sorensen [8] introduced the criterion of the crack tip opening angle (CTOA) for the initiation of propagation of cracks under conditions of plane strain based on previous work. Recently Ogasawara and Okamura [9] have shown that the criterion of a constant CTOA may also be applied to plane-stress problems.

Subsequent experimental studies, especially on metals [10], have shown that, in thin specimens, the final state at the initiation of SCG is mainly a plane-stress state where the plastic zone becomes of the Dugdale type form. However, other experiments with the same materials have shown that for thick specimens at the initiation of SCG and aftewards, a plane-strain diffuse-type of plastic zone is developed [11]. Other experiments have indicated that the CTOA for plane strain remains constant during the SCG phase and in general, the Rice–Sorensen model is consistent with the experimental results, although the experimental measurement of CTOA is quite difficult in natural cracks due to the irregular profile of the zig-zagged fracture surfaces [12, 13]. This difficulty imposed the replacement of CTOA in some tests by the crack opening angle (COA) measured along the whole length of the crack and presents an averaged picture of the opening of the crack flanks [14, 27].

It has been also indicated that the COD and the COD against R curve should be parameters influencing SCG, which are independent from the geometry of the crack and the thickness of the cracked plate, but they depend on the mechanical properties of each material [15].

Whereas many and complete studies of the SCG have been undertaken for metals, this is not the case for polymeric substances. One of the main reasons seems to be the large variety of polymers, which is connected with a large spectrum of variation of their

0022–2461/89 $03.00 + .12

mechanical and physical properties. For certain polymers like polymethylmethacrylate (PMMA) [16, 17] the polymethylene [18, 19] and the epoxy resins [20] many interesting studies have been presented, this is not the case for the polycarbonate (PC), material which has found a variety of applications. Indeed most of the studies on PC are limited to the explanation or the causes of the change of its mechanical properties below the glass transition temperature, T_g, of the material [21], or to study qualitatively or semi-qualitatively the well known phenomenon of crazes in this material [22, 23].

Only a few papers deal with the phenomenon of SCG in PC [24], but in a sense different than that developed for metals.

The aim of this paper is to describe the experimental results obtained by using scanning electron microscopy (SEM) and concerned with the above-mentioned problems related to SCG in PC. Scanning electron microscopy enables the use of small specimens with the advantages of, besides material conservation, experimental convenience and suitable specimen geometries for studying the macro- and micro-mechanisms of the SCG process.

2. Experimental procedure

For the study of the mode of fracture under steady crack growth of ductile materials the polycarbonate of bisphenol A was selected as a convenient polymer since it presents typical properties of an elastic-perfectly plastic material [25]. Single edge-notch tensile specimens (SENT) were prepared for testing in the loading device of the scanning electron microscope. The specimens were of the dogbone type with overall lengths between the jaws of the loading unit equal to $l = 35$ mm. Their width was $w = 4.9$ mm and their thickness varied between $d_{min} = 0.7$ mm and $d_{max} = 3$ mm.

An initial slot of length a varying between 0.5 and 4.5 mm was prepared by cutting the specimens with a razor blade up to the tips of the slots so that in-plane constraint factors a/w were achieved varying between 0.07 and 0.6.

When the specimens were formed one of their lateral faces was coated with a fine aluminium layer by evaporation. The thickness of this layer was of the order of 5 nm which was achieved with the help of a digital film monitor system Edwards Co. type FTM3. Thinner layers were avoided since they frequently created the phenomenon of charging which destroyed the reliability of the tests.

This thin layer also played the role of a highly sensitive tracker of the deformation pattern of the specimen's substrate. Indeed, since the layer possessed a different elastic modulus to that of the specimen and in general much higher than this modulus, the deformation mode of the surface of the specimen induces large elastic deformations to the coating layer which cracks along lines of maximum principal strains. Then, the coating layer is a sensitive indicator and tracker of the strain concentrations in the substrate and an automatic plotter of the slip-line fields around the crack tips.

All tests were executed in a scanning electron microscope of the type Cambridge S4-10 equipped with a special tensile stage. The strain rates applied to all specimens were kept low and equal to $\dot{\varepsilon} = 0.5$ mm min^{-1}. The photographic recording was executed always "on load" with a rate of one frame every 5 sec.

For the quantitative evaluation of the experimental results during slow steady crack growth (SCG) use was also made of the system of TV-scanning video of type REN-Industries Inc. where the maximum speed of recording of the transient phenomena was approximately 1 cm sec^{-1}. Finally, the voltage step used was 20 kV and the beam current 200 μA.

3. Mechanisms of steady crack growth in ductile polymers

We have used as a typical ductile polymer polycarbonate (PC) for our tests a progressive tensile loading of dogbone specimens of different thicknesses containing transverse edge cracks of different initial lengths, a, the following characteristic phases of plastic deformation were detected in the electron scanning microscope.

At the beginning, as the external loading was progressing, phase I developed, during which blunting was established at the vicinity of the crack tip in the form of an ellipse of high ellipticity. At the end of the blunting phase a damaged ligament appeared penetrating the cracked plate from the crack tip at an almost transverse direction. When a critical length of this damaged ligament was established, the phase I of plastic deformation of the specimen was ended.

The next phase II consisted of a progressive propagation of the blunted part of the crack at the expense of the damaged ligament which was progressively exhausted. This phase of steady crack growth by the progressive exhaustion of the damaged ligament was accompanied by the phenomenon of development of slip lines with the form of a "Gorki moustache", independently of the thicknesses of the specimens and the ratios of the initial crack lengths, a, to the widths, w, of the specimens.

Fig. 1a shows the initiation of blunting and the formation of the critical length of the damaged ligament for a cracked PC plate with $d = 1.5$ mm and $a/w = 0.07$. Fig. 1b presents the first step of advancement of the blunted crack at the expense of a part of the initial damaged ligament and the development of the Gorki-type slip-line field. Fig. 1c presents the enlarged detail of the damaged ligament of Fig. 1a.

Fig. 2 presents the same phase II for a cracked plate of the same thickness $d = 1.5$ mm but with different in-plane constraint factor. Again, in Fig. 2a the critical length of the damaged ligament was established and the next three steps of steady crack growth (Figs 2b to d) indicate that they have been achieved at the expense of the damaged ligament which is diminished by steps occupied by the advancing blunted flanks of the crack and, at the end in Fig. 2d, completely exhausted. This is a critical step of the crack propagation which corresponds to the case where an impending really steady crack growth follows.

It is of interest to indicate that the Gorki-moustache type of slip-line field is also developed in this case, which is wider than the previous one of Fig. 1, which,

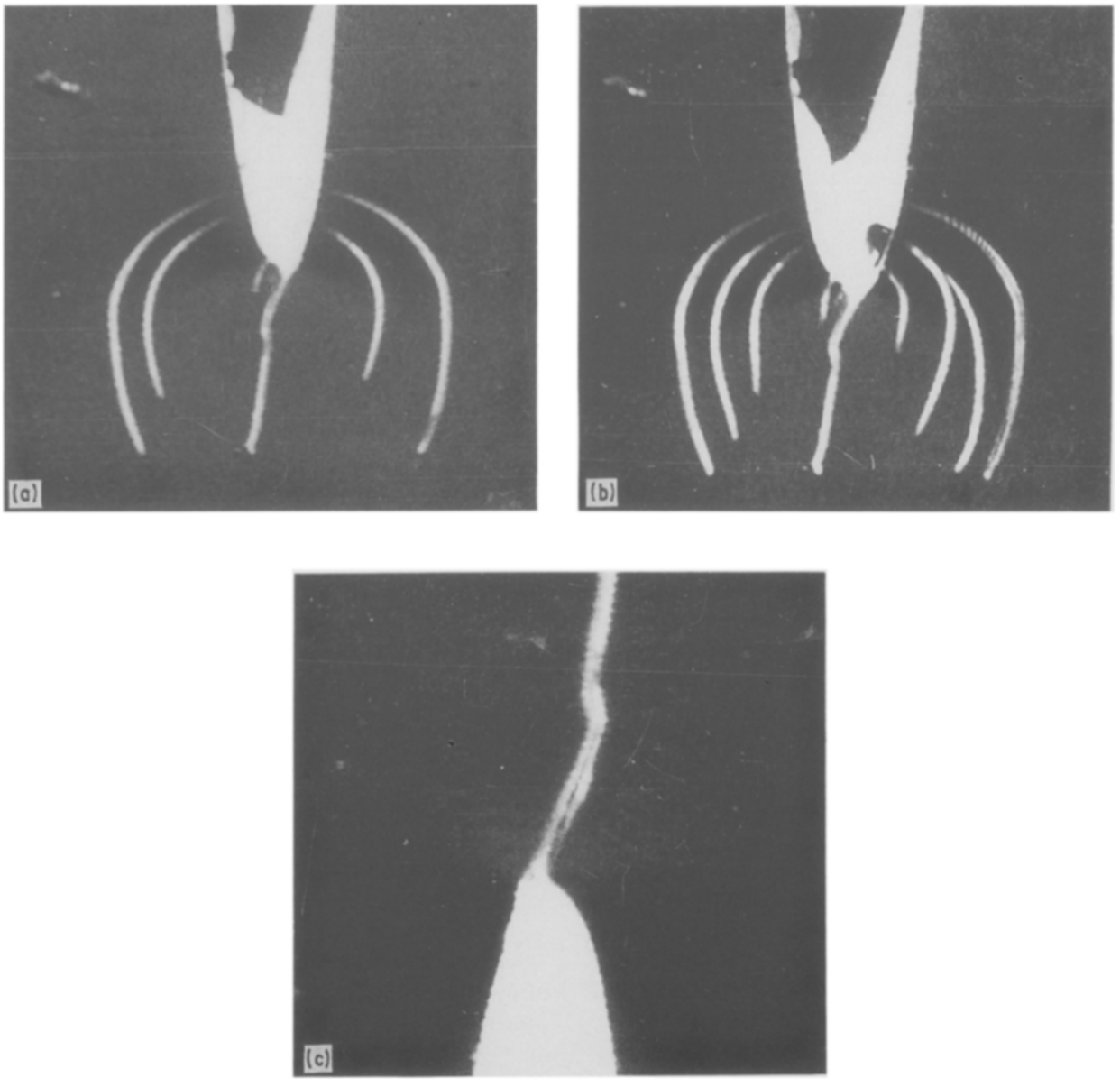

Figure 1 (a, b) The development of the blunted crack and the formation of its damaged ligament in PC at the end of phase I; (×200) (c) Detail of the form of ligament for a mixed state of stress (plane-stress and plane strain) (×800). (d = 1.5 mm, a/w = 0.07).

besides the slip-lines, contains a dense population of crazes, voids and microcavities in the form of elongated ellipsoids, oriented parallel to the one family of the slip lines.

In Fig. 3 the thickness of the cracked plates was reduced to d = 0.7 mm, whereas a/w = 0.1, in order to ascertain better overall plane-stress conditions for the cracked specimen. Again the mechanism of the progressive crack growth by a respective consumption of the already established damaged ligament is apparent. While in Fig. 3a the initial step of the establishment of the critical damaged ligament is shown, in Figs 3b and c the step by step exhaustion of this ligament by the advancement of the blunted crack is apparent. Fig. 3c indicates another critical point of the procedure of SCG in phase II where all the ligament is absorbed by the blunted crack.

In this case where the lateral constraint factor contributes to a typical plane stress slip-line field its form is very different to the slip-line fields of the previous figures with both families of the slip lines apparent, which indicates that the shear strain is equally important in the two principal shear directions. This slip-line field resembles closely with the respective slip-line fields given by Shih [25] and Theocaris [26] when they were studying these fields in cracked plates under plane-stress conditions, either without or with blunting phenomena.

Another important observation is related to the shape of the through the thickness crack profile of the cracked specimens of various thicknesses. It has been consistently observed as with similar cases with metallic specimens that the crack profile for thin specimens is almost straight and normal to the lateral faces of the cracked plate, whereas, as the thickness of the plate is increased, this profile starts to become concave at the initiation of phase II where the damaged ligament appears in front of the crack tip. This concave shape evolves as the loading progresses and tends to become straight with the exhaustion of the damaged ligament. Fig. 4 presents three different transverse sections of cracked specimens along the crack plane, where the

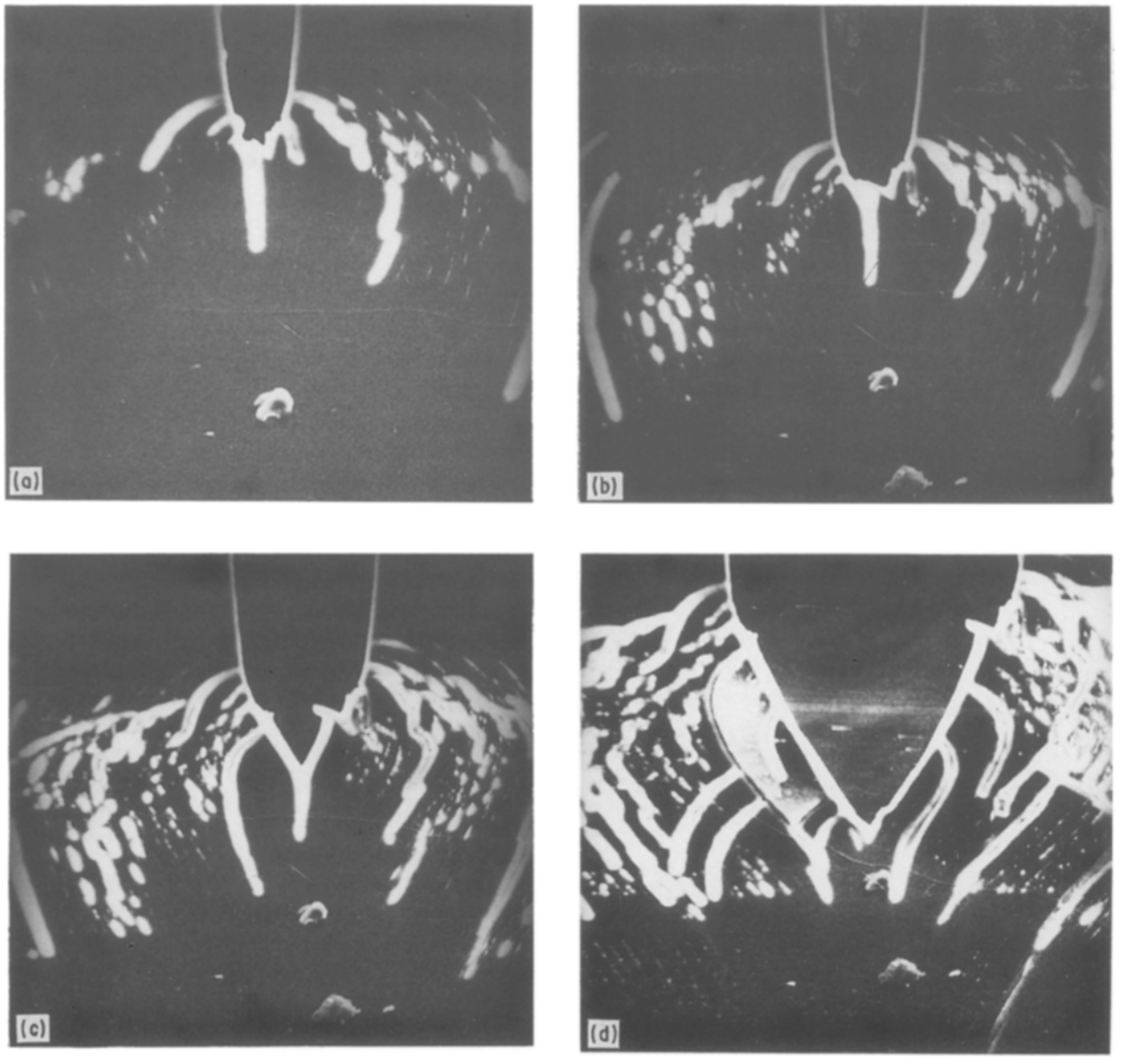

Figure 2 Four successive steps of the advancement of the blunted crack in PC under conditions of plane strain at the expense of the damaged ligament. (d) indicates the critical step where a complete exhaustion of the ligament is attained ($d = 1.5$ mm, $a/w = 0.2$, $\times 200$).

crack profiles are shown for different loading steps.

Figs 4a and b correspond to specimens of the same thickness $d = 3.0$ mm, but of different ratios a/w and therefore different in-plane constraint factors. Fig. 4a has a ratio $a/w = 0.10$ whereas for Fig. 4b $a/w = 0.30$. In both cases the initial concave profiles are apparent, as well as successive evolutions of these profiles in the forms of triangles of increasing height. In the same photos the classical conical markings, which outside the boundary of the concave front are degenerated to river markings, which indicates the existence of a shearing process under development.

On the contrary in Fig. 4c where $d = 1.0$ mm and $a/w = 0.30$, that is the same in-plane constraint factor between specimens of Figs 4b and c, the conical markings are very limited in front of the straight crack front, whereas the few river markings are almost parallel to the lateral phases of the plates. This indicates that the plane-stress mode of loading of the plate presents different characteristics to the respective plane-strain mode.

Now the variation of externally applied load P in the tensile specimens is studied in terms of the increase of the crack length Δa in phase II. We derive the plots shown in Fig. 5 for a constant strain rate $\dot{\varepsilon} = 0.5$ mm min^{-1} and different values of d's and a/w's. The curves plotted for two different thicknesses and two different a/w ratios have similar trends showing a rapid increase of the load P with Δa, which levels out and attains a maximum value for $\Delta a \simeq 200\,\mu$m independent of the thickness and the in-plane constraint factor a/w. Since this length almost coincides with the length of the damaged ligament, it may be concluded that the external load attains its maximum with the exhaustion of the damaged ligament and the end of phase II. Beyond this limit and when the crack enters phase III of the proper stable crack growth the load diminishes smoothly and levels out to some constant value.

It is of interest to evaluate also the variation of the crack-tip opening angle (CTOA) during crack propagation in phases of stable crack growth. Fig. 6 presents the evolution of CTOA in terms of the length Δa. The increase of CTOA in thin and thick specimens

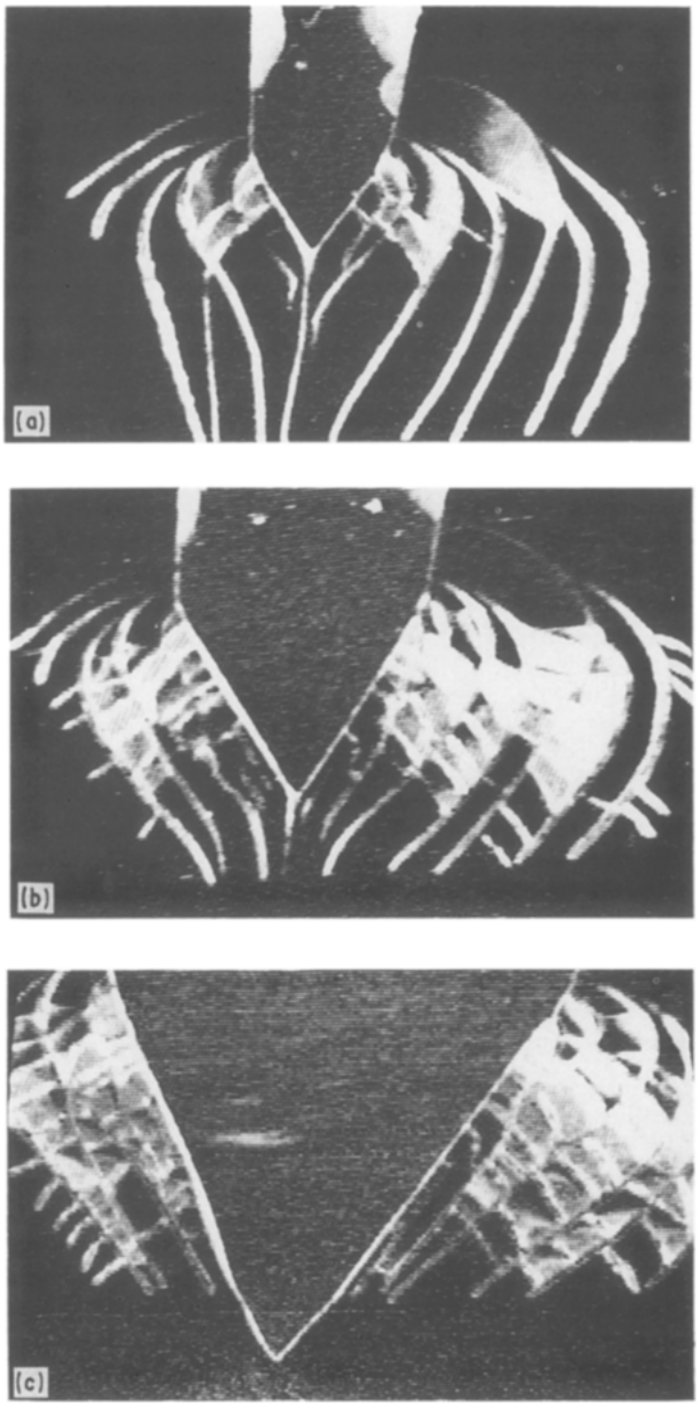

Figure 3 Three successive steps of the same process for a PC specimen under plane-stress conditions ($d = 0.7$ mm, $a/w = 0.1$, $\times 500$).

is developed in different manners. This fact is indicated in Figs 2 and 3. Indeed, in thick specimens where the crack profile is in general concave the accurate evaluation of CTOA is difficult since it varies along the thickness of the plate. In these cases we may speak about an effective value of CTOA averaging the values measured at different depths of the specimen. In order to obtain the individual values for CTOA very accurately in thick specimens repeated measurements were executed at different positions through the thickness of the plate with the aid of the TV-video facility of the scanning electron microscope at high magnifications. These average values were plotted in Fig. 6. On the contrary, for thin specimens under plane-stress conditions the flanks of the cracks and the damaged ligaments were almost straight and well defined and the evaluation of the respective CTOAs was much easier and more accurate.

Two typical cases were plotted in Fig. 6 where the variation of CTOA with the advancement Δa of the crack was shown. While the plane-stress blunted crack develops very rapidly and smoothly, its blunting, and therefore its crack-tip opening angle, the case of fracture dominated by plane strain with thicker specimens presents a considerable time lag in the development of their CTOAs which start to increase almost at the end of the phase of progressive crack tip advancement by consumption of respective lengths of the damaged ligament.

However, both cases exemplified by the respective

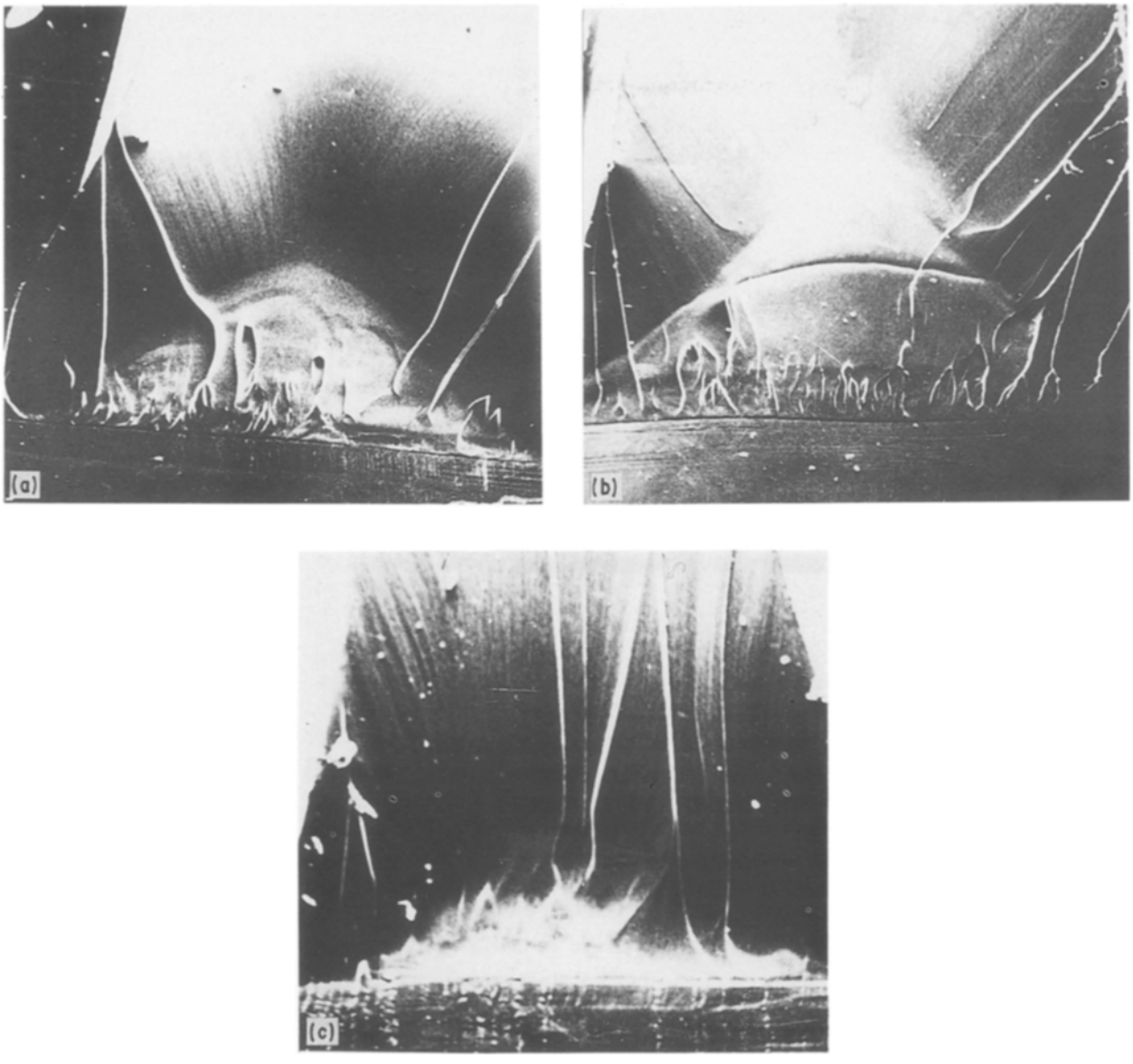

Figure 4 Transverse sections of cracked PC-specimens along the crack plane indicating typical propagation steps (a, b) for plane strain and (c) plane stress. ((a) $d = 3.0\,\text{mm}$, $a_0/w = 0.10 \times 50$, (b) $d = 3.0\,\text{mm}$, $a_0/w = 0.30 \times 50$, (c) $d = 1.0\,\text{mm}$, $a_0/w = 0.30 \times 80$.)

plottings in Fig. 6, attain a limiting plateau for their values of CTOA at 55°. This phenomenon was general and appeared in a large number of tests.

It is of interest to point out that a small pseudophase appeared frequently at the end of phase II and the beginning of the proper stable crack growth phase III, where the values of the CTOA presented an insignificant but consistent bell-shaped jump instability for this angle before they attained their asymptotic value in phase III. This pseudophase was indicated also in Fig. 6. However the maxima of these bell shaped curves did not exceed 3° to 5° and may be attributed to the phenomenon of resilience at the end of the rapidly increasing CTOA at phase II.

4. The proper stable crack growth phase

The transition from the progressive crack growth at the expense of successive parts of the damaged ligament to the proper stable crack growth is made smoothly but it is distinct and happens at a crack prolongation of $\Delta a = 200$ to $250\,\mu\text{m}$ when the totality of the damaged ligament is transformed into a blunted crack.

Fig. 4 indicates clearly that at this stage the externally applied load after passing a maximum value levels off at some lower value sufficient to maintain the steady propagation of the stable crack growth. Similarly the values of CTOA stabilize at a limiting value of 55°.

In the stable crack growth phase the crack propagates in a different mode, where both its flanks are forwarded along the crack axis and simultaneously are moved sidewards, so that its flanks maintain their respective value of the established CTOA.

Fig. 7 presents a series of three photographs where the already completely established blunted crack in phase II advances under constantly maintained load by forward and simultaneous sideward movements. The traces of the successive lips of the crack are clearly shown in each photograph and any instantaneous position in each photograph indicates a constancy in the value of CTOA. The thickness of this particular

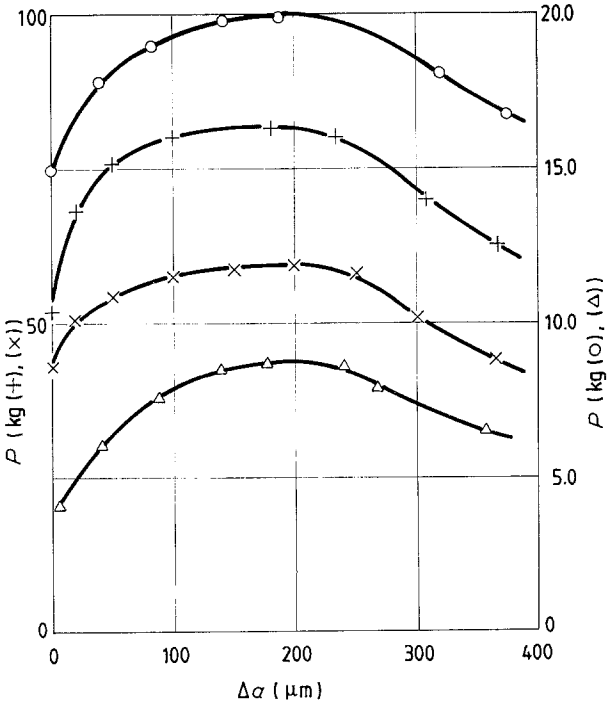

Figure 5 The variation of the externally applied load P plotted against the crack length during the stable crack growth phases ($\times$ $a/w = 0.07$, $d = 2.0$ mm; $+$ $a/w = 0.15$, $d = 2.0$ mm; $\circ$ $a/w = 0.07$, $d = 0.7$ mm; Δ $a/w = 0.45$, $d = 0.7$ mm, strain rate $\dot{\varepsilon} = 0.5\,\text{mm}\,\text{min}^{-1}$).

specimen is $d = 1$ mm and the in-plane constraint factor $a/w = 0.1$.

In this SCG phase the phenomenon of development of slip-line fields around the crack does not appear and only the traces of the successive flanks of the advancing crack are marked. It is clear from these photographs that the CTOA remains constant as is also indicated in Fig. 6 for phase III.

Fig. 8 presents the variation of the crack speed plotted against the increase of the crack length for two typical cases, that is for almost plane-strain conditions (upper curve; inclined crosses) and for plane-stress conditions (lower curve, triangles). It is clear from this plot that the crack velocities present a constant rate which is smaller for phase II where the crack tip advances at the expense of the existing damaged ligament and higher for the proper stable crack growth phase III. The instability in the slope of the two straight lines of either curve is accompanied by the instability of the CTOA which presents in this transition zone a bell shaped variation.

Finally, it is worthwhile stating that the speed rates are insensitive to the variation of the thickness of the specimens and therefore independent of the lateral and the in-plane constraint factors.

Fig. 9 presents another aspect of the mechanism of advancement of ductile fractures in the stable crack growth. This figure shows the variation of the crack opening displacement, COD, plotted against the advancement of the crack tip, Δa, for different in-plane and lateral constraint factors. It is clear from this figure that for phase II COD is increasing linearly and independently of the above constraint factors whereas for phase III there is a marked difference in slope between thin and thick specimens with the thin specimens having smaller slopes than their thicker counterparts.

The form of curves in Fig. 9 indicates clearly that the so-called tearing modulus [14] expressed by

$$T_\delta = \frac{E}{\sigma_0} \times \frac{\mathrm{d}\delta}{\mathrm{d}a} \tag{1}$$

where σ_0 is the yield stress of the material in simple tension and $\mathrm{d}\delta/\mathrm{d}a$ expresses the increment of the COD for an increase of the crack propagation length $\mathrm{d}a$ remains a constant quantity in the phase of stable crack growth, and it is very small of the order of 50, as compared with other ductile materials [27]. This difference constitutes a characteristic property of polycarbonate which, although it is very ductile, presents a rather lower resistance to tearing than other ductile materials. One of the main causes of this reduction in the tearing resistance of PC should be the intense viscoelastic behaviour of the material. For the same reason the values of CTOA for this material is much larger than for other ductile materials [14] and it is also larger than the respective COA in phase III of the stable crack growth, a fact which is in disagreement with other experimental results [14].

5. Results

It is clear from the experimental results presented in this paper that both phases studied belong to the stable crack growth (SCG) type since no phenomena

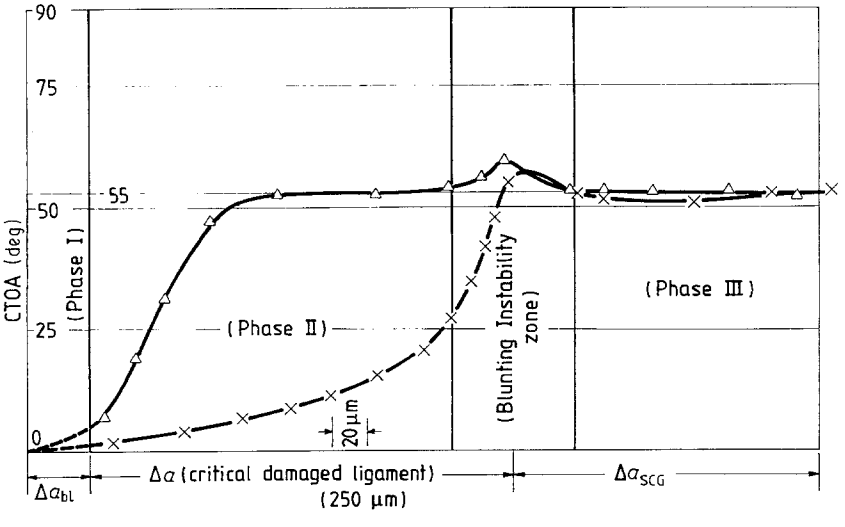

Figure 6 The variation of CTOA plotted against crack length for two typical cases of stable crack growth in PC specimens under plane stress (Δ) and plane strain ($\times$) conditions.

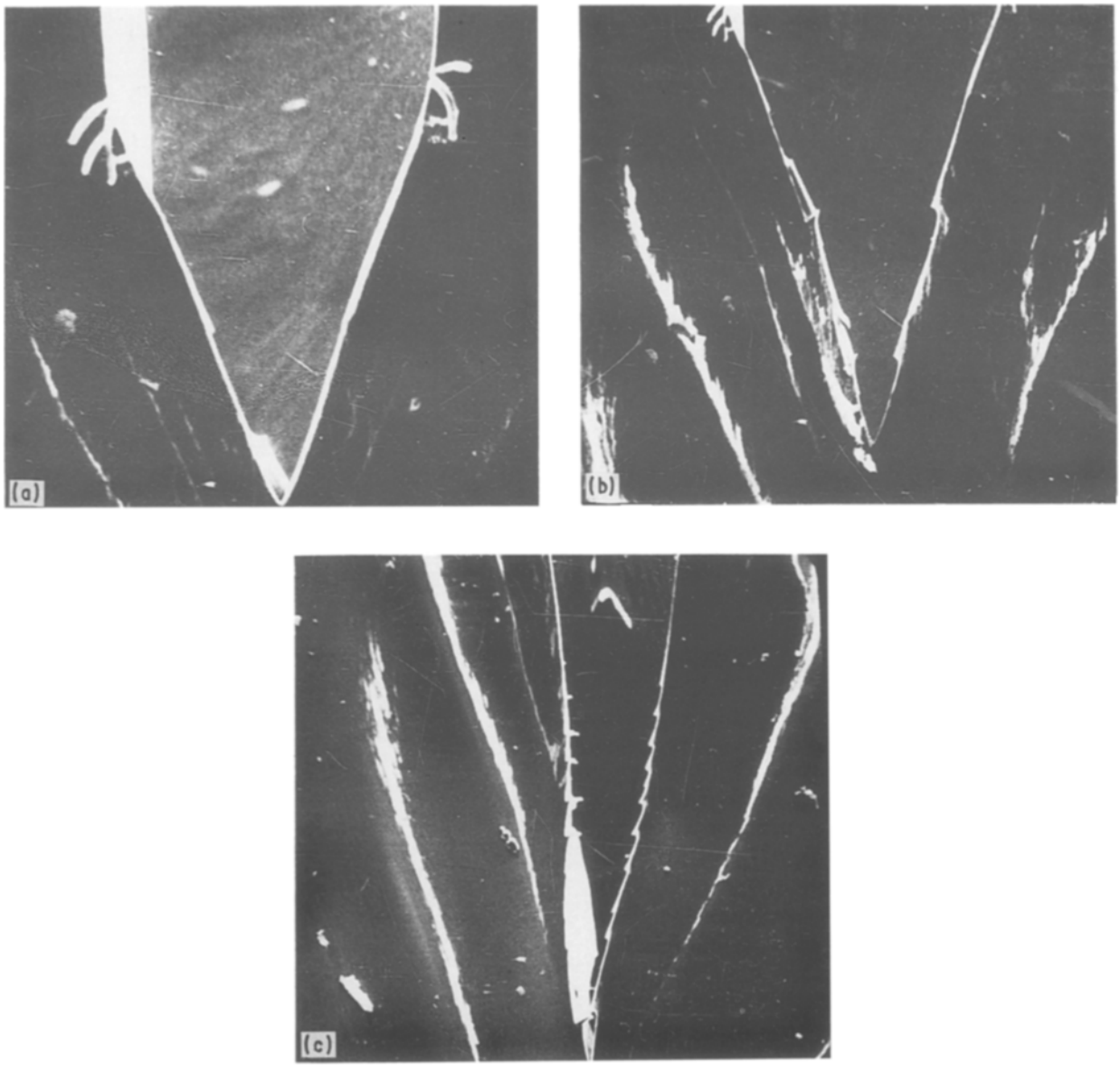

Figure 7 Successive steps of the crack advancement under constant CTOA and COA at the phase III of stable crack growth in PC specimens with $d = 1\,\text{mm}$, $a/w = 0.1$ ($\times 50$).

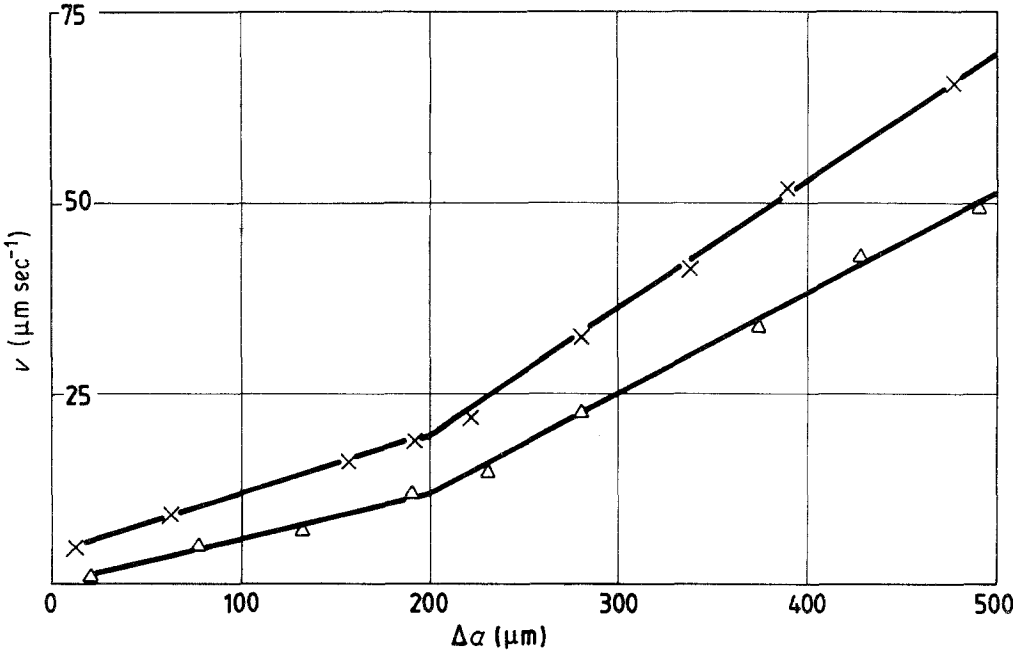

Figure 8 The variation of crack velocity, V, plotted against crack length during the two phases of the stable crack growth of PC specimens under conditions of plane stress and plane strain. (Strain rate $\dot{\varepsilon} = 0.5\,\text{mm}\,\text{min}^{-1}$, $\times$ $d = 3.0\,\text{mm}$, $a/w = 0.4$; Δ $d = 0.7\,\text{mm}$, $a/w = 0.4$).

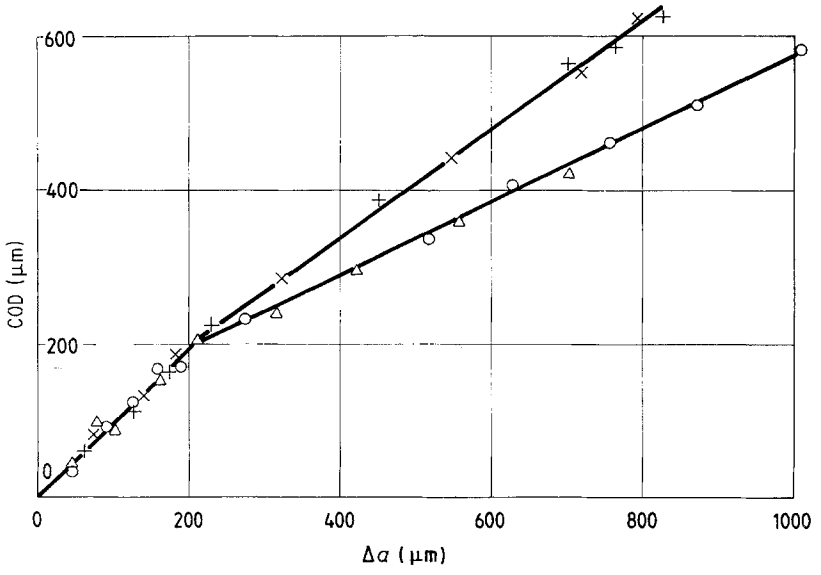

Figure 9 The variation of COD plotted against crack length during the two phases of the stable crack growth of PC specimens under conditions of plane stress and plane strain. (○ $d = 0.7$ mm, $a/w = 0.05$; Δ $d = 0.7$ mm, $a/w = 0.50$; + $d = 2.0$ mm, $a/w = 0.07$; × $d = 2.0$ mm, $a/w = 0.45$).

of self-propagating cracks were detected. The main difference between the precursor phase II, where the crack growth occurs by consuming the already established damaged ligament in front of the crack, from the proper SCG-phase III, is in the propagation velocity of the crack.

The appearance of the damaged ligament along the crack axis in front of the crack in phase I, which is a transition zone of evolution of blunting and development of this ligament is reminiscent of the Dugdale model which indicates a plane-stress state of stress. This confirms the remark made by Gerberich and coworkers [17], where it is stated that many polymers present the tendency to behave according to the Dugdale model without the prerequisite of a small thickness.

Since for PC there are no studies concerning the influence of the thickness and the geometry of the specimen on the different parameters of SCG, our tests have shown that by changing the lateral constraint factor (thickness) and the in-plane constraint factor (a/w ratio) we can pass from a plane-strain to a purely plane-stress condition.

An important result derived from this study is that the critical length Δa_c of the damaged ligament is insensitive to these factors remaining always of the order $\Delta a_c \approx 200\,\mu$m.

A clear indication from Figs 2 and 3 is that thick specimens are under predominant plane-strain conditions, whereas thin ones are under plane stress. The crack profile is concave for plane strain, whereas for plane stress it is almost straight and normal to the lateral faces. These experiments indicate a different behaviour to the remarks in reference [24] that the plane strain conditions do not favour the development of viscoelastic phenomena as much as plane-stress conditions do. However, it is obvious also from our tests that a plane-stress condition engenders a much more uniform distribution of the ingoing energy along the whole length of the damaged ligament and thus forces the crack profile during the phase of the exhaustion of the damaged ligament to take a straight line form with the result of the well behaved development of the crack propagation.

On the contrary the large lateral constraint factor for plane-strain conditions imposes a concentration of the ingoing energy in the middle of the crack profile which results in a retardation of the smooth development of the CTOA and causes the crack to advance less smoothly than previously. This has a result of changing the form of the damaged ligament which for plane-strain conditions is shorter and wedge-like discontinuity developed in an irregular mode, whereas for plane-stress conditions this ligament is long, fibrous and regular.

Furthermore, for plane-strain conditions where the crack profile is generally concave the length of the filament is variable along the thickness of the cracked plate and therefore it is necessary to define an effective length for this quantity.

All these differences in the form of the crack profile the damaged ligament and other characteristic quantities appearing during SCG are elegantly demonstrated in Figs 4a to c where in the two first photographs plane-strain crack profiles are presented whereas in Fig. 4c the plane-stress case was exhibited. The bright triangles in Figs 4a, b indicate the regions dominated by plane-strain conditions. Inside these triangles the main concave zone of plane-strain is strikingly shown. Inside this zone the conical markings are radially and uniformly disposed, which outside the curved concave fronts degenerate into river markings due to shear loading which may correspond to dimples appearing in the same places in metallic specimens and therefore they are indications of a triaxial ductile fracture.

These luminous zones clearly indicate that the lateral constraint factor influences much more intensively the state of stress at the crack front than the variation of the in-plane constraint factor measured by the a/w ratio, since in Fig. 4c where plane-stress conditions prevail the conical markings are rather sparse and concentrated at the centre of the crack front, where some small plane-strain conditions emerge. Moreover, the river markings in this case are almost parallel to the lateral faces of the cracked plate.

These observations are in agreement with the remarks by Parvin and Williams [24] that in PC the K_I-fracture toughness is influenced strongly by the

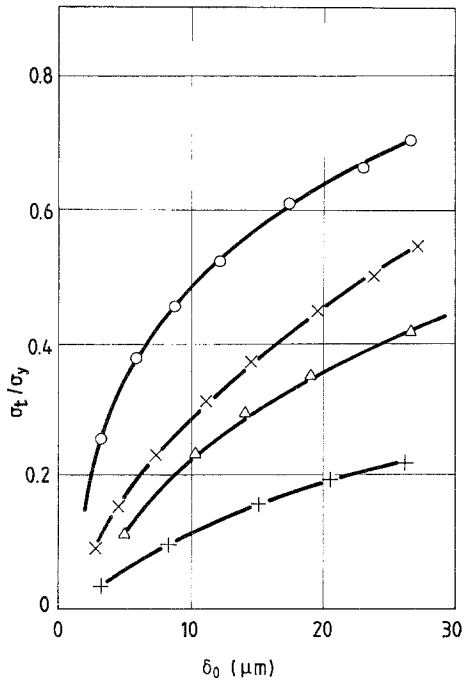

Figure 10 The variation of the applied true stress σ_t, normalized to the σ_y-stress of yielding under tension plotted against the crack opening displacement δ_0. (○ $a/w = 0.1$, $d = 2.0$ mm; Δ $a/w = 0.6$, $d = 2.0$ mm; + $a/w = 0.05$, $d = 0.7$ mm; × $a/w = 0.6$, $d = 0.7$ mm).

thickness variation of the cracked plate. On the other hand this variation of K_I does not influence at all the mode of development of the phase of the progressive consumption of the damaged ligament and its characteristic properties.

This result is corroborated by the photographs of Fig. 7 where the step-by-step propagation of the crack indicates, according to the Dugdale model as developed by Ogasawara and Okamura [9], that the state of stress at the crack tip is plane-stress. This model does not contradict the results given previously concerning the constancy of CTOA during the proper stable crack growth. Indeed the same model indicates that a state of plane stress should create a constant value of CTOA during the SCG.

Fig. 10 presents the variation of the applied true stress, σ_t, normalized to the true stress at the end of the blunting phase I before entering the precursor SCG-phase II, σ_y, plotted against the crack opening displacement, δ_0, for the four typical cases studied in the tests. All four curves approach very closely to parabolae, a fact which is valid only for the Dugdale model, that is if the specimens are under plane-stress conditions. This fact agrees with results by Theocaris [26] in PC where the analysis of the slip-line fields around the edge cracks with blunting was studied. The existence of plane-stress conditions in these plates was shown when the thickness of the plates was reduced.

Fig. 11 presents the rate of exhaustion of the damaged ligament in terms of the relative stress applied to the specimen. One of these curves is based on the theoretical model introduced by Howard and Otter [28] concerning the formation of the plastic zone in front of a stationary crack which is of the Dugdale model type. By an adaptation of this model using a

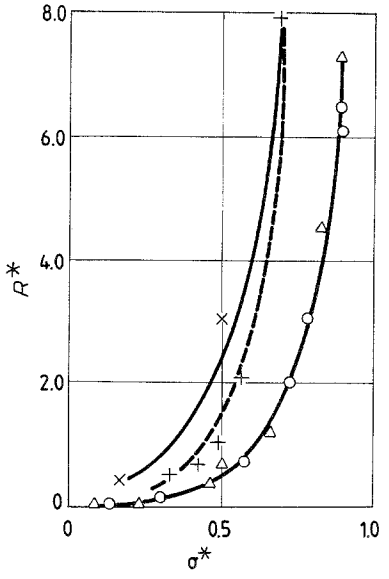

Figure 11 The variation of toughness resistance R^* plotted against the normalized applied stress σ^* for typical plane stress and plane strain specimens of PC in the stable crack growth zone. (+ $a/w = 0.07$, $d = 20$ mm, × $a/w = 0.40$, $d = 20$ mm; ○ $a/w = 0.07$, $d = 0.7$ mm; Δ $a/w = 0.40$, $d = 0.7$ mm).

convenient transformation in which the R^* ordinate is expressed by

$$R^* = \frac{\Delta a_t}{\Delta a_t - \Delta a_i} - 1 \qquad (2)$$

where R^* is the specific work of fracture in the process zone at the crack tip or fracture toughness and Δa_t and Δa_i are the initial total damaged ligament at the beginning of phase II and the consumed part of the ligament at each step of crack propagation in phase II, whereas the σ^* abscissae are expressed by

$$\sigma^* = \left(\frac{\sigma_t}{\sigma_{ti}} - 1\right) \qquad (3)$$

where σ_t is the true stress applied to the specimen at the step considered and σ_{ti} is the initial true stress applied at the beginning of phase II.

In the same figure the $R^* = f(\sigma^*)$ curve was also plotted as derived from the Howard and Otter model [28]. It is clear that for thin specimens, where plane-stress conditions dominate, the coincidence between our experimental results and the Howard–Otter parabola is remarkable, independently of the varying values of the in-plane constraint factor.

On the contrary for thick specimens with plane-strain conditions prevailing the experimental results although they follow similar parabolic curves, they present discrepancies from the H–O model and different slopes for different values of a/w ratios.

6. Conclusions

From the extensive experimental study of stable crack flows in edge-cracked ductile polycarbonate specimens the following conclusions may be drawn.

(i) The SCG step of crack propagation is divided into two distinct phases the SCG by progressive exhaustion of the damaged ligament (phase II) and the proper stable crack growth (phase III).

(ii) The stable crack growth phase by progressive

exhaustion of the damaged ligament presents the following characteristics. There is always an effective crack length covered by this phase which corresponds to the total length of the previously developed damaged ligament in front of the blunted crack. This length is constant for PC and of the order of 200 to 250 μm.

During this phase the crack profile is influenced by the thickness of the specimen and the lateral constraint factor. This profile changes from a concave shape for plane-strain conditions to a flat normal to the faces of the crack profile for plane-stress conditions.

(iii) The CTOA is changing at a different mode during phase II depending on the state of stress of the plate. This quantity attains a limiting plateau attained in phase III of a proper stable crack growth where the value of CTOA is larger than the respective value of COA.

(iv) An instability bell-shaped variation joins the curves of CTOA plotted against crack length at the transition zone from phase II to phase III.

(v) Polycarbonate is a polymer whose fracture takes place to a great extent under prevailing conditions of plane-stress. This conclusion was derived by an extensive study and proof that fractures of PC for any thickness tend to resemble typical fractures described by the Dugdale model.

(vi) Then, a convenient model describing stable crack growth in PC may be a model consisting of a plastic furrow of the Dugdale type penetrating inside a diffuse plastic enclave around the crack tip.

References

1. D. BROCK, *Int. J. Fract. Mech.* **4** (1968) 19.
2. G. GREEN and F. J. KNOTT, *J. Mech. Phys. Solids* **23** (1975) 167.
3. R. G. YODER and C. A. GRIFFIS, ASTM STP 590 (American Society for Testing and Materials, Philadelphia, 1976) p. 61.
4. J. N. ROBINSON and A. S. TETELMAN, Dritte Int. Tagung über den Bruch April 1973 Teil III, (VDI Publisher, Germany) paper 11-421.
5. J. R. RICE, "Mechanics and Mechanism of Crack Growth" (Proceedings Conference at Cambridge, U.K., 1973) edited by M. J. May (British Steel Corporation Physical Metallurgy Centre Publication, Sheffield, 1973) p. 14.
6. G. P. CHEREPANOV, *Int. J. Solids Structure* **4** (1968) 811.
7. D. C. DRUCKER and J. R. RICE, *Engng Fract. Mech.* **1** (1970) 577.
8. J. R. RICE and E. P. SORENSEN, *J. Mech. Phys. Solids* **26** (1978) 163.
9. M. OGASAWARA and H. OKAMURA, *Engng Fract. Mech.* **18** (1981) No. 4.
10. G. T. HAHN and A. R. ROSENFIELD, *Acta Metall.* **13** (1965) 293.
11. G. T. HAHN, A. R. ROSENFIELD and M. SARRATE, "Inelastic Behaviour of Solids" (1970) (McGraw-Hill, New York) p. 673.
12. J. C. LAUTRIDOU and A. PINEAU, *Int. J. Fract.* **17** (1981) R115.
13. S. J. GARWOOD and C. E. TURNER, *ibid.* **14** (1978) R195.
14. C. F. SHIH, H. G. DE LORENZI and W. R. ANDREWS, ASTM STP 668 (American Society for Testing and Materials, Philadelphia, 1979) p. 65.
15. L. A. SIMPSON and C. F. CLARKE, ASTM STP 668 (American Society for Testing and Materials, Philadelphia, 1979) p. 613.
16. G. P. MARSHALL, L. H. COUTTS and J. G. WILLIAMS, *J. Mater. Sci.* **9** (1974) 1409.
17. S. J. ISRAEL, E. L. THOMAS and W. W. GERBERICH, *ibid.* **14** (1979) 2128.
18. N. S. BROWN and S. K. BHATTACHARYA, *ibid.* **20** (1985) 4553.
19. LU XICI and N. BROWN, *ibid.* **21** (1986) 2423.
20. D. C. PHILLIPS, J. M. SCOTT and M. JONES, *ibid.* **13** (1978) 311.
21. G. ALLEN, D. C. W. MORLEY and T. WILLIAMS, *ibid.* **8** (1973) 1449.
22. P. L. CORNES, I. C. SMITH and R. N. HAWARD, *J. Polym. Sci. Polym. Phys. Edn.* **15** (1977) 955.
23. M. D. ATHENE and J. E. KRAMER, *J. Mater. Sci.* **16** (1981) 2967.
24. M. PARVIN and J. G. WILLIAMS, *ibid.* **10** (1975) 1883.
25. F. C. SHIH, PhD thesis, Harvard University, Cambridge, Massachusetts (1973).
26. P. S. THEOCARIS, *J. Engng Fract. Mech.* **31** (1988) 255.
27. M. SAKA, T. SHOJI, H. TAKAHASHI and H. ABÉ, ASTM STP 803 (American Society for Testing and Materials, Philadelphia, 1983) p. 130.
28. I. C. HOWARD and N. R. OTTER, *J. Mech. Phys. Solids* **23** (1975) 139.

Received 1 June
and accepted 13 September 1988